Spatial frequency and fractal complexity in single-to-triple beam holograms

E. I. SCARLAT, M. MIHAILESCU[*], A. SOBETKII[a]
Physics Department, University "POLITEHNICA" Bucharest, 313 Spl. Independentei, 060042 – Bucharest, Romania,
[a]*"OPTICOAT ltd.", 3 Racari Str., Bucharest, Romania*

A new method of assessing the efficiency and uniformity of particular application of a single-to-triple beam conversion for obtaining structured beam configurations is investigated. Conversion efficiency and signal uniformity in the object space are related to the fractal properties in the DOE spatial frequencies as revealed by the multifractal spectrum (MFS), and the associated complex microstructure measured by the Lempel-Ziv complexity (LZC). By directly evaluating MFC and LZC in the DOE plane one can have a complementary instrument when designing phase holograms. These quantities are furnishing valuable technological information for the manufacturing stage: higher values for MFS require greater imprinting finesse, precision, and control, while higher values for LZC need more gray levels, more complex algorithms and more processing resources. In the exploitable range for optical tweezers applications there were revealed correlations of the pairs MFS↔efficiency and LZC↔uniformity. Experimental implementation qualitatively confirms the computational simulations.

1. Introduction

The aim to produce low cost, highly controlled structured beams for optical interconnections [1], lithographic fabrication of photonic crystals [2], or biological microscopy [3] is requiring holographic methods to generate the appropriate diffractive optical elements (DOEs); particularly, the obtaining of continuously shaped beam or stepped multiple-beam of spatially controlled phase and/or intensity distribution for optical tweezers purposes is a promising way to effectively handling the biological tissues down to the sub-cellular level.

Here a new method of assessing several properties of a single-to-triple beam conversion is investigated. Conversion efficiency and signal uniformity in the object plane are related to the fractal properties in the DOE – i.e. Fourier – plane in terms of the coarseness of the underlying spatial frequencies as revealed by the multifractal spectrum (MFS), and the associated complex microstructure measured by the Lempel-Ziv complexity (LZC).

The structure of the study is as follows: Sect.2 is briefly mentioning the principle of DOE design and simulation, and the relevant quantities as well; Sect.3 is presenting the results and the subiacent comments; finally, the concluding remarks are reviewing the main findings and original contributions.

2. Theoretical background

2.1 DOE simulation and experiment

In the stepped multiple-beam approach used in the present work, the phase DOEs are designed to split the energy of the unique incident beam in three but only three emerging rays. DOEs were generated by an iterative Fourier transform algorithm (IFTA) implemented with MatLab software [4] by imposing constraints on *i)* output signal configuration S_{object} i.e. three emerging spots in the object space; *ii)* conversion efficiency, defined as the ratio between the intensity in the signal window and the intensity in the whole matrix in the object space whose ideal value tends to one; *iii)* uniformity of the intensities – in the sense of the ratio of the sum of the intensities in the first order to the intensity of the central spot. For equal intensities the uniformity is of 67%. The central ray is zero-order diffracted while the nearest two are of order one. They are fully symmetrical with respect to the central one. The diffracted energy in the following orders should be zero.

Briefly, in the Fraunhofer approximation, the unknown transfer function t_{DOE} of the hologram is the solution of an integral equation of the form

$$S_{object}(x_0, y_0, z) \sim \frac{\exp(ikz)}{i\lambda z} \exp\left[\frac{ik}{2z}\left(x_0^2 + y_0^2\right)\right] \times$$
$$\times \int t_{DOE}(x, y, 0) \exp\frac{-2i\pi(x_0 x + y_0 y)}{\lambda z} dx dy, \quad (1)$$

where S_{object} is the output constraint on the field distribution, λ the wavelength and $k=2\pi/\lambda$ the wavenumber of the input field restricted to a circular aperture, (x,y) and (x_0,y_0) the coordinates in the DOE and object plane, respectively, and z the distance between the DOE and object planes.

The dependence on the varying parameters namely the central spot diameter D and the inter-spot distance L of MFS, LZC, conversion efficiency and signal uniformity are investigated. Whatever the space – object or Fourier – of the analyzed quantity, L and D are expressed in pixels in the *object* space. One should note that overlapping of the beams $L<D$ is allowed and the corresponding region $L/D<1$ is the most interesting for optical tweezers.
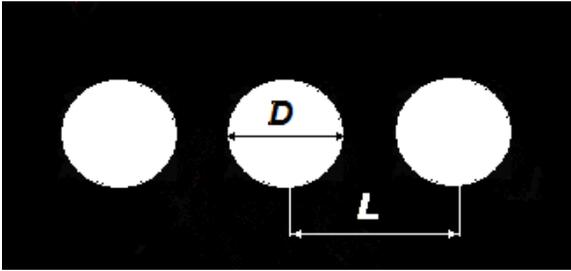

Fig.1. Signal window in triple beam configuration: central spot diameter D, and inter-spot distance L.

2.2 Multifractal spectrum

When dealing with the matrix version of DOE it is easy to create the 1-dim sequence of its lines (columns) in order to obtain a series of samples $\{s(n)\}_{n=1,N}$ whose the standard multifractal detrended fluctuation analysis (MF-DFA) can be applied [5]. The series are of more than $N=15,000$ data points each. Usually, the richness of multifractal spectra can be evaluated in terms of the difference $\Delta\alpha=\alpha_{max}-\alpha_{min}$, where α_{max} and α_{min} are the extreme values of the Hölder exponents α that characterize the irregularities of the data points in the series [6]:

$$\left| s(n) - P_m\left(n - n_0\right) \right| \le C\left|n - n_0\right|^\alpha \qquad (2)$$

In Eq.(2) P_m is the polynomial of order m that approximates the series in the current point s_n, and C is a constant. The larger $\Delta\alpha$, the broader the spectrum. Since there are difficulties in computing the extreme values, here the multifractal spectrum is evaluated as the deviation from a monofractal structure [7]

$$\delta = \alpha_0 - H. \qquad (3)$$

In Eq.(3) α_0 is the Hölder exponent assigned to the greatest fractal dimension $\alpha_0\leftrightarrow f(\alpha_0)$ of the subsets, while H is the Hurst exponent [8].

Most software packages are directly providing the bell shaped pattern $(\alpha, f(\alpha))$ with the possibility of finding the coordinates of any point on the curve, including its maximum, so that α_0 could be easily found; on the other side, the Hurst exponent is also available in packages using MF-DFA, or might be easily computed by locally software; FracLab package is providing such tools.

2.3 Lempel-Ziv complexity

To compute LZC, the numerical sequence of data has to first be transformed into a binary sequence consisting of only two symbols: 0 and 1. This is achieved by comparing the data with a threshold, usually the median and whenever the signal is larger than or equal to the threshold the particular data is replaced by 1, otherwise by 0. The next step is parsing the obtained symbolic sequence i.e. identifying the number of distinct words present in the sequence. The complexity counter is given by the number of distinct patterns contained in the sequence. Details on the parsing procedure can be found in [9].

Here the normalized LZC is computed: it gives the complexity of a string relative to that of a genuinely random one. As the length approaches infinity, the normalized LZC index approaches unity. A very complex, noise-like experimental series could have LZC index slightly larger than unity because of the finite length. Hereafter LZC is denoting the normalized index. The computation is performed using the Chaos Data Analyzer [10].

All quantities are evaluated for simulations only. Finally, the DOE were implemented and verified on a spatial light modulator (SLM).

3. Results and discussion

Based on IFTA simulations, the conversion efficiency and signal uniformity in the object space are compared with MFS and LZC of the corresponding DOEs for several values of L and D. The variation of MFS is shown in Fig.2. It exhibits a knoll along the plane $L=D$. The valley in the region $L/D<1$ is softer than in the opposite one $L/D>1$.
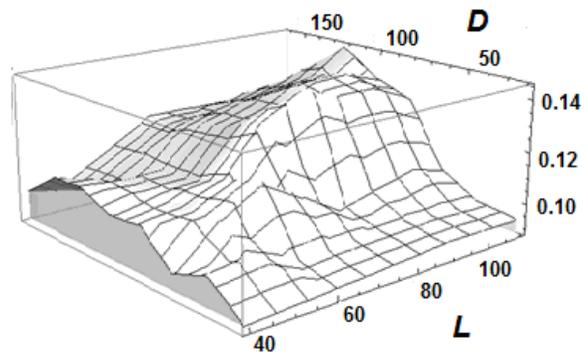

Fig. 2. MFS dependence on central spot diameter D, and inter-spot distance L.

Even the other quantities are not following similar variations, there are portions of intervals revealing similar behaviours; such an example is shown in Fig. 3. Apart from the local maxima, the trends are supporting the fact that light scattering improves on more irregular and consequently "more multifractal" diffractive gratings [11].
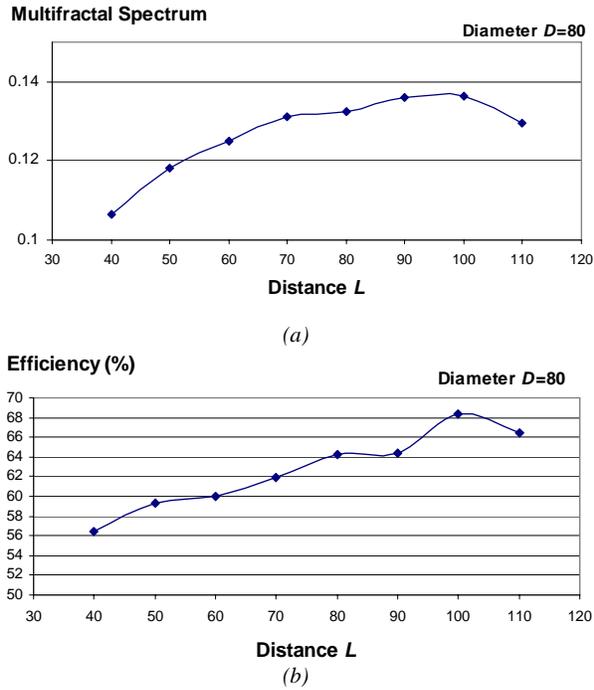
Multifractal Spectrum

Diameter *D*=80

(a)

Efficiency (%)

Diameter *D*=80

(b)

Fig. 3. MFS (a) and efficiency (b) vs. inter-spot distance.

According to the graphs above, one can correlate the efficiency with MFS, especially in the case of DOEs that are closer to monofractal structure (see Fig. 4).
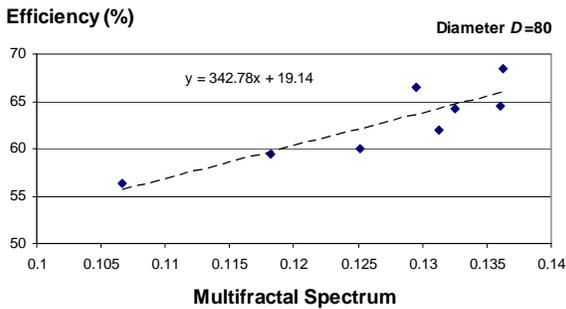
Efficiency (%)

Diameter *D*=80

$$y = 342.78x + 19.14$$

Fig. 4. Underlying relation between conversion efficiency and MFS.

Analogously, but depending on the spot diameter, another similarity between LZC and uniformity is shown in Figs. 5 and 6.

Higher values for LZC indicate diminished correlations. Apart from the periodicity induced by the

consecutive lines of the matrices, the loosing of correlations is the consequence of the whitening of the signal in the inner data content of every line of the matrices. Not surprisingly, the uniformity tends also to follow LZC: the Fourier transform of uniform top hat distributions in the object space are satisfactory approximated by Gaussians in the DOE space; to the limit – still far in the present cases –, when narrowing the hat toward the Dirac-like pulse, the Gaussian extend toward the white noise characterized by LZC tending to unity.

By eliminating the spot diameter one can obtain the image of the underlying relation between uniformity and LZC.
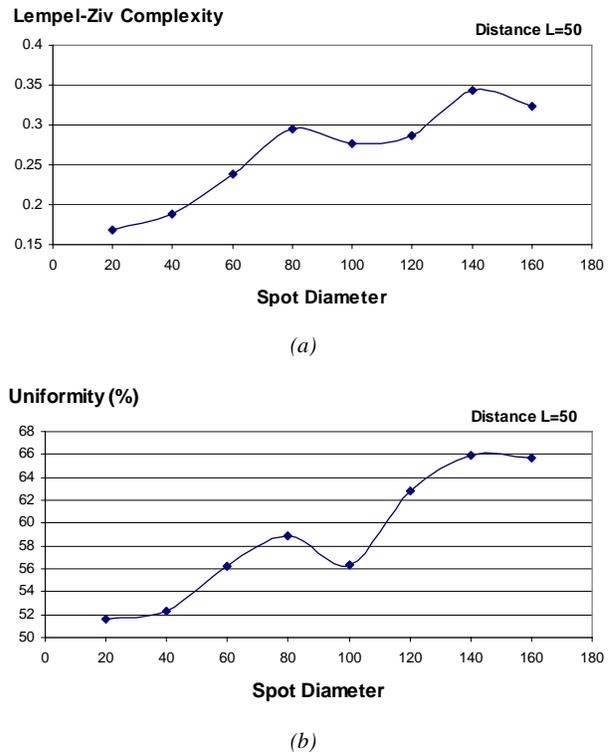
Lempel-Ziv Complexity

Distance L=50

(a)

Uniformity (%)

Distance L=50

(b)

Fig. 5. LZC (a) and uniformity (b) vs. central spot diameter.

Uniformity (%)

Distance *L*=50

$$y = 84.836x + 36.253$$

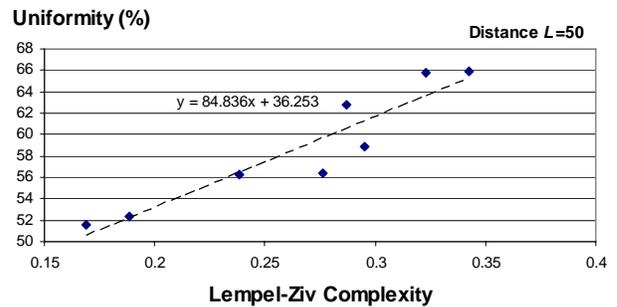*Fig. 6. Underlying relation between uniformity and LZC.*

There are not positive correlations among the other pairs MFS↔uniformity and LZC↔efficiency; on the contrary there, is an apparently weak anticorrelation between LZC – and consequently uniformity – on one side, and efficiency, on the other side, when comparing Fig. 5 (a) and Fig. 7 (a).
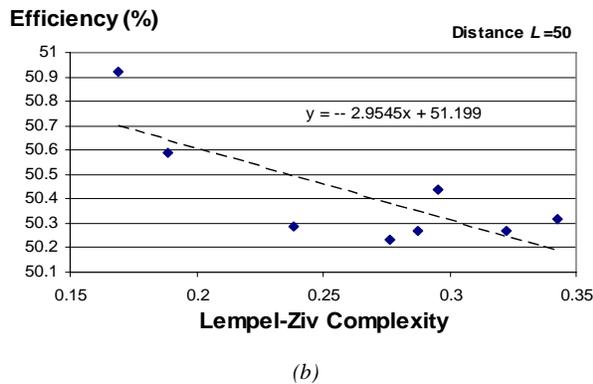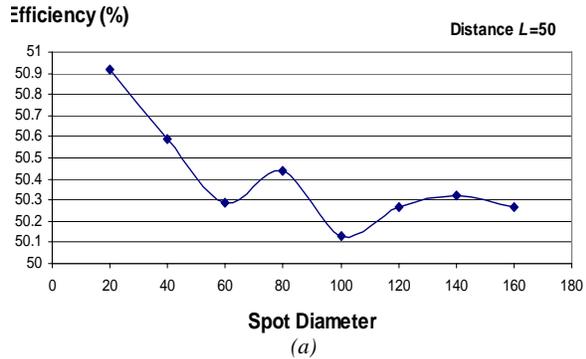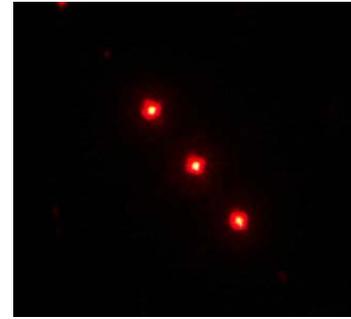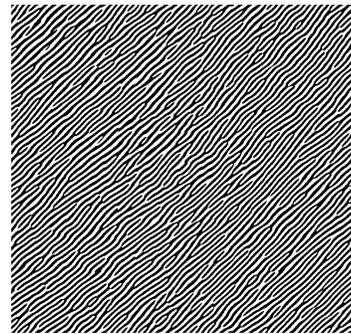

(a)

(b)

Fig. 7. Efficiency vs. central spot diameter (a), and anti-correlation between LZC and efficiency (b).

Generally, the increase of the pattern complexity makes the dependences uncontrollable, especially in the upper range when LZC is approaching the unity. However, for lower values, as the case, the result has to be taken cautiously. The variations are small and more investigations are necessary.

The experiments were then performed with a SLM model Sony LCX016AL coupled to the appropriate computational hardware. The real triple beam grabbed with a commercial CCD camera and its corresponding DOE are shown in Fig.8 for the case of equal intensities. Uniformity and efficiency are qualitatively approaching the simulations mainly because of the top hat approximation.

(a)

(b)

Fig. 8. Triple beam (a), and the corresponding IFTA generated hologram (b).

4. Conclusions

A method of assessing some properties of a single-to-triple beam conversion is investigated by relating conversion efficiency and signal uniformity to the fractal properties in spatial frequency domain namely MFS and LZC. In the exploitable range for optical tweezers applications i.e. $0.5 < L/D < 1.5$ there were revealed correlations of the pairs MFS-efficiency and LZC-uniformity.

By directly evaluating MFC and LZC in the DOE plane one can have a complementary instrument when designing phase holograms. These quantities are furnishing valuable technological information in the manufacturing stage: higher values for MFS require greater imprinting finesse, precision, and control, while higher values for LZC need more gray levels, complex algorithms and processing resources.

It is not possible to have a global optimum i.e. maximum uniformity, minimum LZC and MFC.

The analyses were performed on simulated quantities when synthesizing DOEs in order to get appropriate intensity distributions, with maximum efficiency; the uniformity remains subject to the particular application. The experimental implementations are satisfactory fitting the simulations.

References

[1] M. Mihailescu, A. M. Preda, D. Cojoc, L. Preda, E. I. Scarlat, J. Optoel. Adv. Mat. **9**, 2485 (2007).

[2] L. P. Biro, Z. Balint, K. Kertesz, Z. Vertesy, G. I. Mark, Z. E. Horvath, et al. Phys. Rev. E **67**, 021907 (2003).

[3] A. Lafong, W. J. Hossack, J. Arlt, T. J. Nowakowski, N. D. Read, Opt. Express **14**, 3065 (2006).

[4] M. Mihailescu, A. M. Preda, D. Cojoc, E. I. Scarlat, L. Preda, J. Optoel. Adv. Mat. **9**(4), 1071 (2007).

[5] J. W. Kantelhardt, S. A. Zschiegner, A. Bunde, S. Havlin, E. Koscielny-Bunde, H. E.Stanley, Physica A **316**(87), 87 (2002).

[6] D. B. Percival, A. T. Walden, Cambridge Univ. Press, Cambridge, 2000.

[7] E. I. Scarlat, M. Mihailescu, A. Preda, L. Preda, Proc. EOS on Diff. Opt., 227-228, Barcelona, 2007.

[8] H. E. Hurst, Trans. Am. Soc. of Civil Eng. **116**, 770 (1951).

[9] J. Hu, J. Gao, J. C. Principe, IEEE Trans. Biomed. Eng. **53,** 2606 (2006).

[10] J. Sprott, G. Rowlands, Phys. Acad. Software Man. 69, 1997.

[11] B. Hou, G. Xu, W. Wen, G. K. L. Wong, Appl. Phys. Lett. **25**(85), 6125 (2004).

_____
[*]Corresponding author: mona_m@physics.pub.ro